Electronic Supplementary Material (ESI) for CrystEngComm.

SUPPORTING INFORMATION

Halogen-bonded cocrystals of N-salicylidene Schiff bases and iodoperfluorinated benzenes: hydroxyl oxygen as halogen bond acceptor

Andrea Carletta[a], Marija Zbačnik[b], Matea Vitković[b], Nikolay Tumanov[a], Vladimir Stilinović*[b], Johan Wouters*[a] and Dominik Cinčić*[b]

[a]Department of Chemistry, NISM, University of Namur, 61 rue de Bruxelles, B-5000 Namur, Belgium. E-mail: johan.wouters@unamur.be
[b]Department of Chemistry, Faculty of Science, University of Zagreb, Horvatovac 102a, HR-10002 Zagreb, Croatia. E-mail: dominik@chem.pmf.hr, vstilinovic@chem.pmf.hr

TABLE OF CONTENTS

1. Results of Single Crystal X-ray experiments

Table S1 General and crystallographic data for compound (**I**)(**14tfib**).

Molecular formula	$(C_{13}H_{11}NO)(C_6F_4I_2)$
M_r	599.09
Temperature / K	298
Crystal system	triclinic
Space group	*P*–1
***a* / Å**	5.3298(5)
***b* / Å**	5.9839(4)
***c* / Å**	15.276(2)
***α* / °**	90.196(8)
***β* / °**	93.824(9)
***γ* / °**	100.428(7)
***V* / Å³**	478.01(8)
Z	1
D_{calc} **/ g cm⁻³**	2.081
λ**(Mo**K_α**) / Å**	0.71073
μ **/ mm⁻¹**	3.335
Crystal size / mm	0.40 x 0.21 x 0.08
***F*(000)**	282
Refl. collected/unique	2079/1592
No. of restraints	92
Parameters	190
$R[F^2 \geq 2\sigma(F^2)]$	0.0448
$wR(F^2)$	0.0896
Goodness-of-fit, *S*	0.994
CCDC No.	1854281

Table S2 General and crystallographic data for compounds (**II**)(**13tfib**) and (**II**)$_2$(**14tfib**).

Molecular formula	$(C_{12}H_{10}N_2O)(C_6F_4I_2)$	$(C_{12}H_{10}N_2O)_2(C_6F_4I_2)$
M_r	600.08	798.30
Temperature / K	295(2)	295(2)
Crystal system	triclinic	monoclinic
Space group	$P\bar{1}$	$P2_1/c$
a / Å	7.2968(5)	15.3516(5)
b / Å	15.2068(12)	5.75781(16)
c / Å	19.3646(15)	16.8675(6)
α / °	110.783(7)	90
β / °	91.701(6)	105.671(3)
γ / °	100.999(6)	90
V / Å^3	1960.9(3)	1435.53(8)
Z	4	4
D_{calc} / g cm^{-3}	2.033	1.847
λ(MoK_α) / Å	0.71073	0.71073
μ / mm^{-1}	3.254	2.252
Crystal size / mm	0.540 x 0.250 x 0.050	0.530 x 0.340 x 0.330
F(000)	1128	772
Refl. collected/unique	9739/7450	3999/3169
No. of restraints	0	0
Parameters	490	193
$R[F^2 \geq 2\sigma(F^2)]$	0.0323	0.0299
$wR(F^2)$	0.0638	0.0622
Goodness-of-fit, S	1.019	1.033
CCDC No.	1854282	1854283

Table S3 General and crystallographic data for compounds (**II**)(**135tfib**) and (**II**)$_2$(**135tfib**).

Molecular formula	$(C_{12}H_{10}N_2O)(C_6F_3I_3)$	$(C_{12}H_{10}N_2O)_2(C_6F_3I_3)$
M_r	707.98	906.20
Temperature / K	295(2)	295(2)
Crystal system	orthorhombic	monoclinic
Space group	*Pbcn*	$P2_1/c$
a / Å	24.1738(4)	4.1899(3)
b / Å	9.45562(19)	29.106(2)
c / Å	17.8360(3)	24.6798(18)
α / °	90	90
β / °	90	92.834(7)
γ / °	90	90
V / Å^3	4076.92	3006.1(4)
Z	8	4
D_{calc} / g cm^{-3}	2.307	2.002
λ(MoK_α) / Å	0.71073	0.71073
μ / mm^{-1}	4.637	3.173
Crystal size / mm	0.392 x 0.367 x 0.138	0.550 x 0.080 x 0.070
F(000)	2608	1720
Refl. collected/unique	6209/5069	4955/3884
No. of restraints	0	0
Parameters	248	384
$R[F^2 \geq 2\sigma(F^2)]$	0.0247	0.0465
$wR(F^2)$	0.0501	0.0742
Goodness-of-fit, S	1.039	1.118
CCDC No.	1854279	1854280

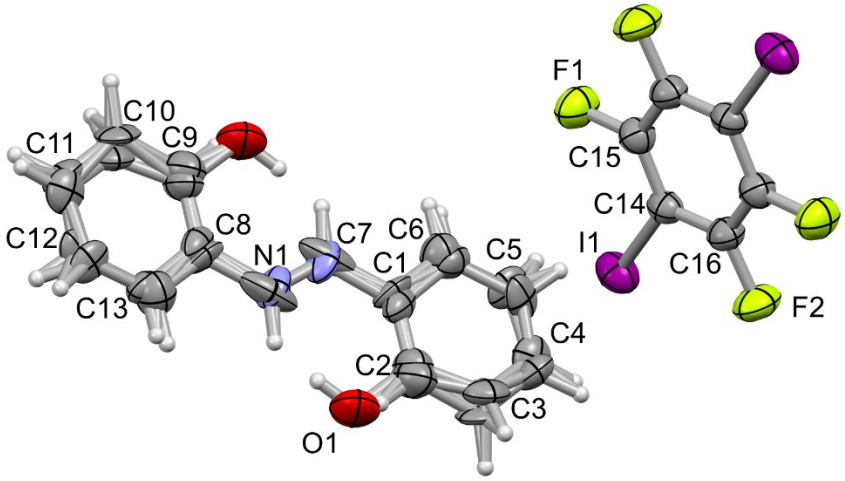

Figure S1. Molecular structure of (**I**)(**14tfib**) showing the atom-labelling scheme. Displacement ellipsoids are drawn at the 40 % probability level, halogen bonds are marked with blue dashed lines, and H atoms are shown as small spheres of arbitrary radius.

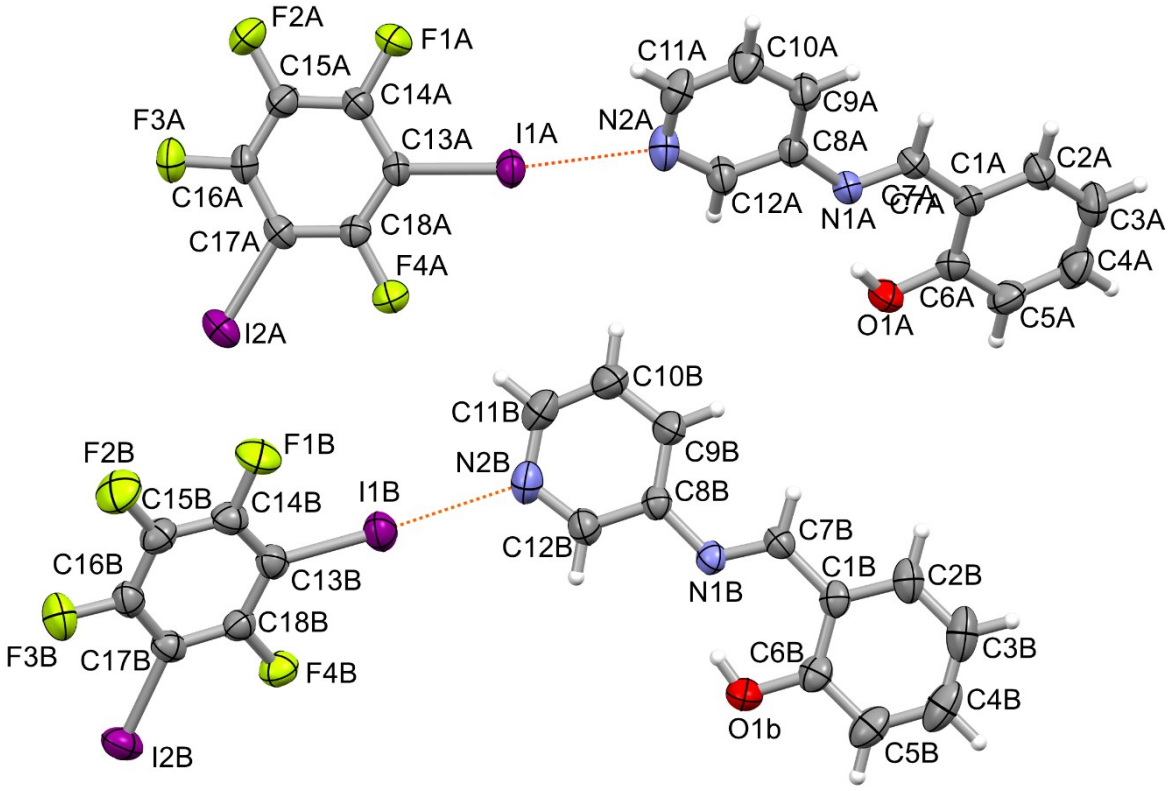

Figure S2. Molecular structure of (**II**)(**13tfib**) showing the atom-labelling scheme. Displacement ellipsoids are drawn at the 40 % probability level, halogen bonds are marked with blue dashed lines, and H atoms are shown as small spheres of arbitrary radius.

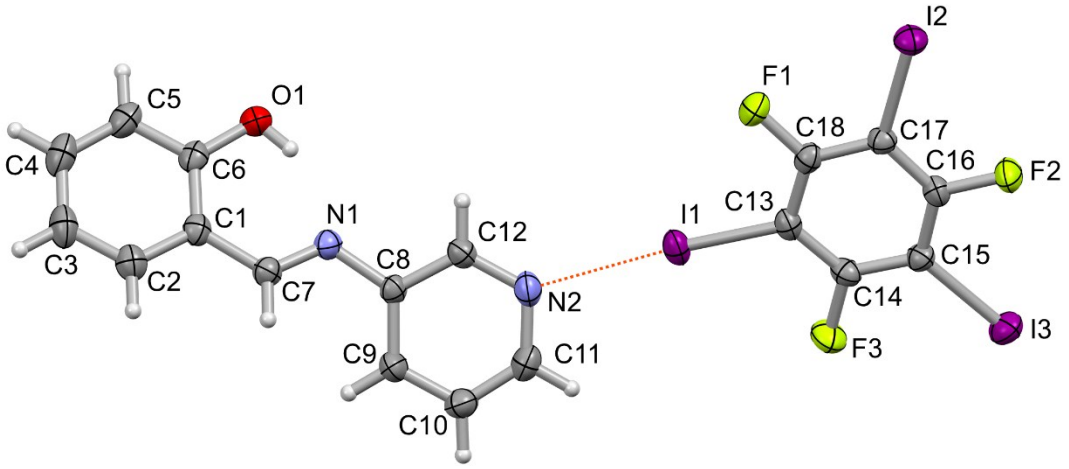

Figure S3. Molecular structure of (**II**)(**135tfib**) showing the atom-labelling scheme. Displacement ellipsoids are drawn at the 50 % probability level, halogen bonds are marked with blue dashed lines, and H atoms are shown as small spheres of arbitrary radius.

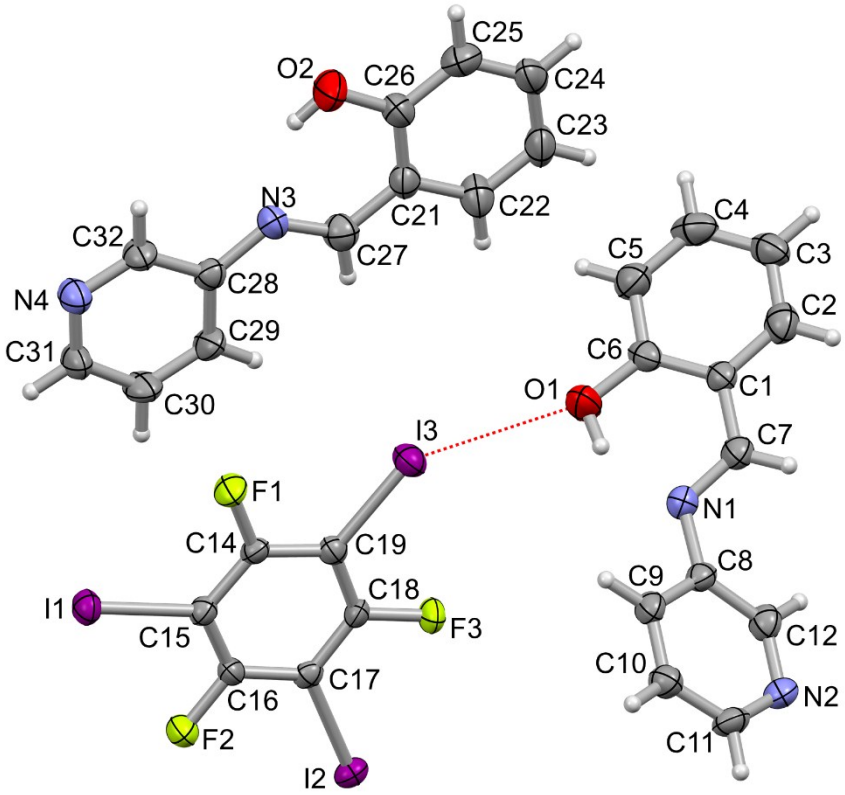

Figure S4. Molecular structure of (**II**)$_2$(**135tfib**) showing the atom-labelling scheme. Displacement ellipsoids are drawn at the 50 % probability level, halogen bonds are marked with blue dashed lines, and H atoms are shown as small spheres of arbitrary radius.

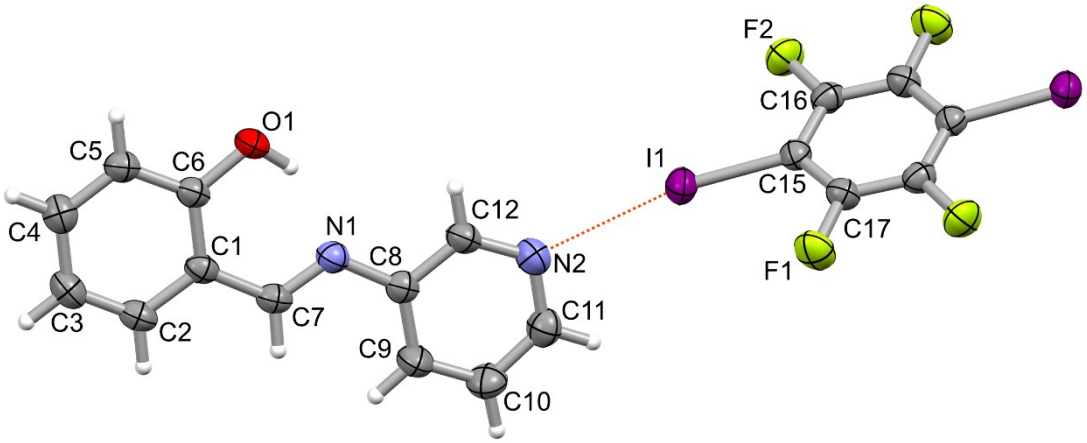

Figure S5. Molecular structure of (**II**)$_2$(**14tfib**) showing the atom-labelling scheme. Displacement ellipsoids are drawn at the 50 % probability level, halogen bonds are marked with blue dashed lines, and H atoms are shown as small spheres of arbitrary radius.

Table S4 The Hirshfeld surface analysis for cocrystals of Schiff bases with the selected four halogen donors; the percentage of Hirshfeld surface of the donor molecule corresponding to contacts with halogen atoms.

	I···X	I···N	I···O	I···H	I···C	I···I
(I) (14tfib)	39,2	0	0	14,4	12,7	0
(II) (13tfib)	32,6	4,3	3,5	21,1	0,8	0,7
	31	4,3	3,2	15,5	2,6	0,6
(II) $(14tfib)_2$	36	5,5	0	25,1	0,4	0
(II) (135tfib)	48,3	2,8	3,1	24,3	6	7,2
(II) $(135tfib)_2$	49,8	5,7	3,7	30,5	3,6	3,8
iwomue	33,8	0	11,2	19	0,2	3,5
iwonuf	33,4	0	7,5	18,5	3,1	0
iwopan	39,3	0	11,8	23	1,2	3,3
sedfuf	36,3	0	10,5	19,7	0	2,5
sedgoa01	37,1	0	10,2	20	0,7	6,1
vazloa	32,8	0,3	9,6	12,5	3,4	2,6
vazmiv	35	0,2	7,1	14,2	7,1	3,8
vazmuh	29,4	0	9,1	12,8	2,5	0,9
vaznao	28,7	0	8	20,6	0	0

2. Results of PXRD experiments

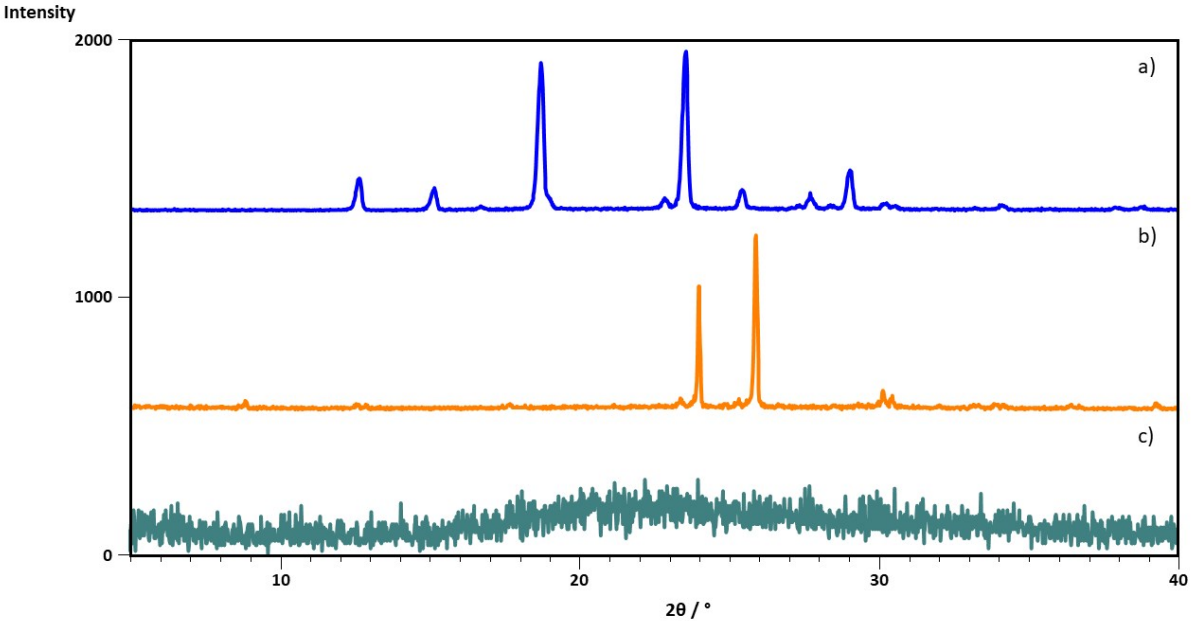

Figure S6 The PXRD patterns of a) **I**, b) **12tfib** and c) the powder product of grinding **I** and **12tfib** (1:1).

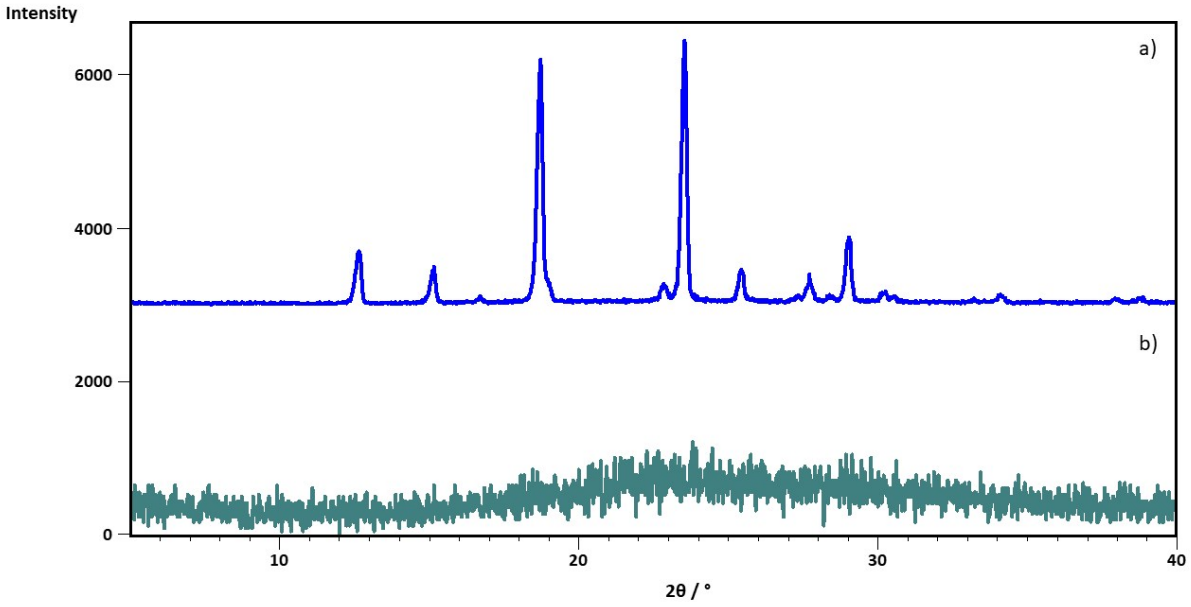

Figure S7 The PXRD patterns of a) **I** and b) the powder product of grinding **I** and **13tfib** (1:1).

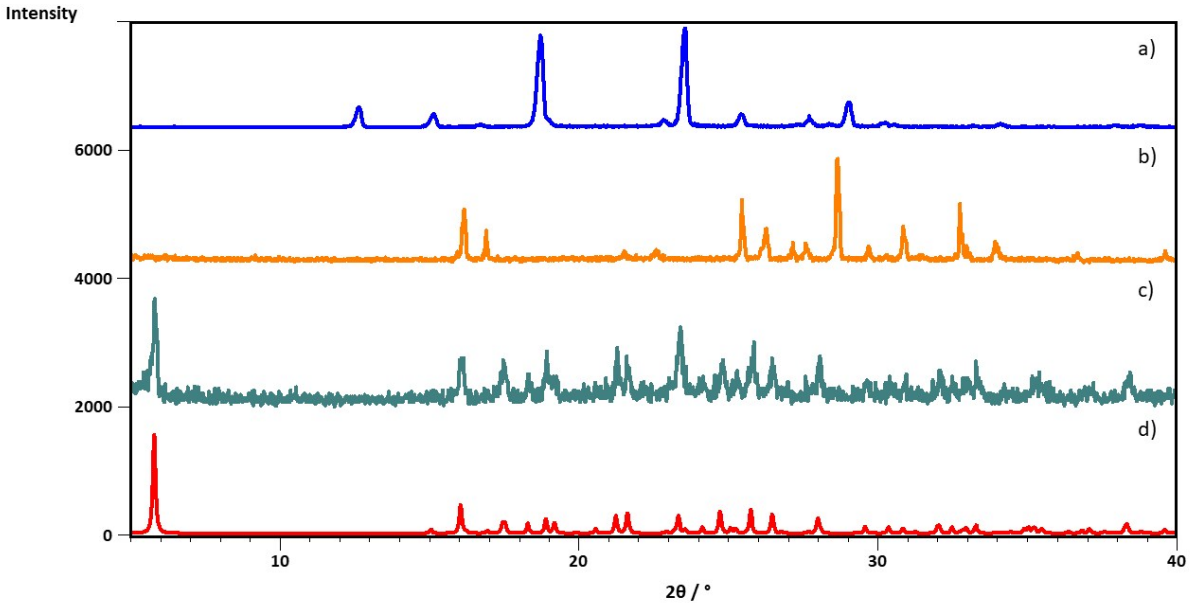

Figure S8 The PXRD patterns of a) **I**, b) **14tfib**, c) the powder product of grinding **I** and **14tfib** (1:1) and e) the calculated PXRD pattern of **(I)(14tfib)**.

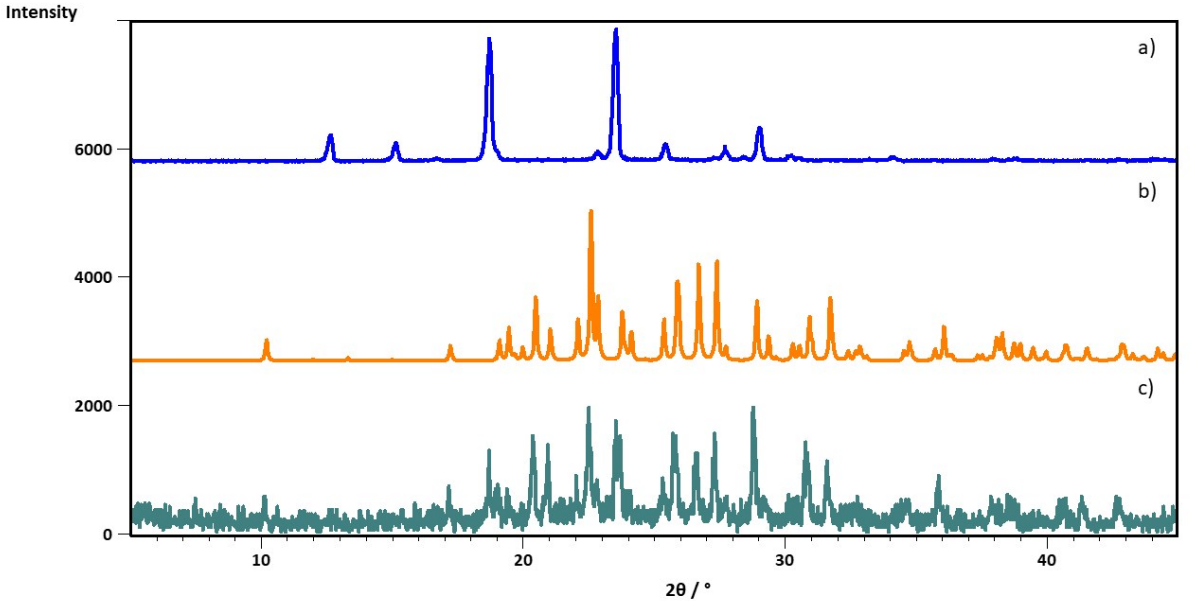

Figure S9 The PXRD patterns of a) **I**, b) **135tfib** and c) the powder product of grinding **I** and **135tfib** (1:1).

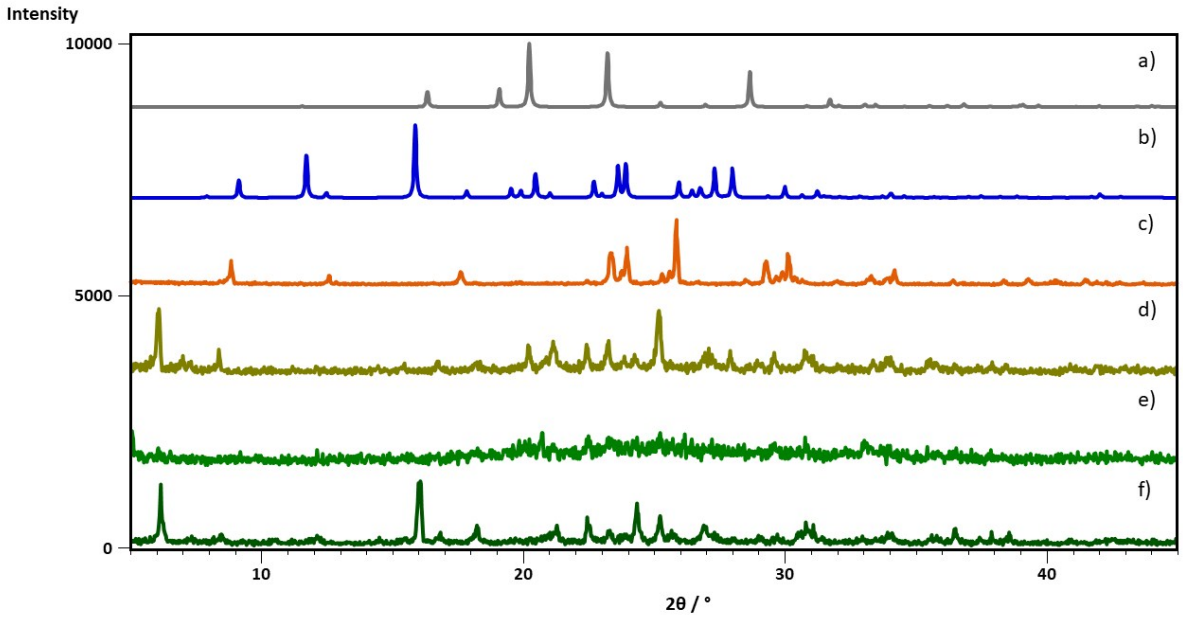

Figure S10 The PXRD patterns of a) **amp**, b) **II**, c) **12tfib**, d) the powder product of grinding **sal**, **amp** and **12tfib** (1:1:1), e) the powder product of grinding **sal**, **amp** and **12tfib** (2:2:1) and f) the powder product of grinding **sal**, **amp** and **12tfib** (2:2:1) left in the ambient conditions for 2 weeks.

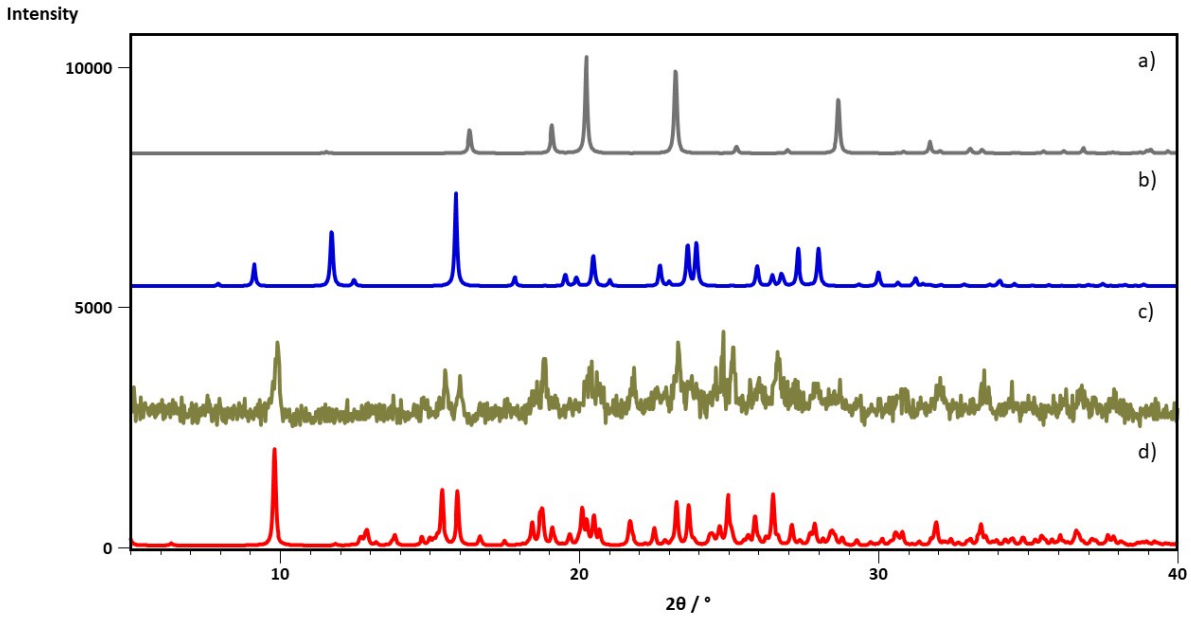

Figure S11 The PXRD patterns of a) **amp**, b) **II**, c) the powder product of grinding **sal**, **amp** and **13tfib** (1:1:1) and d) the calculated PXRD pattern of **(II)(13tfib)**.

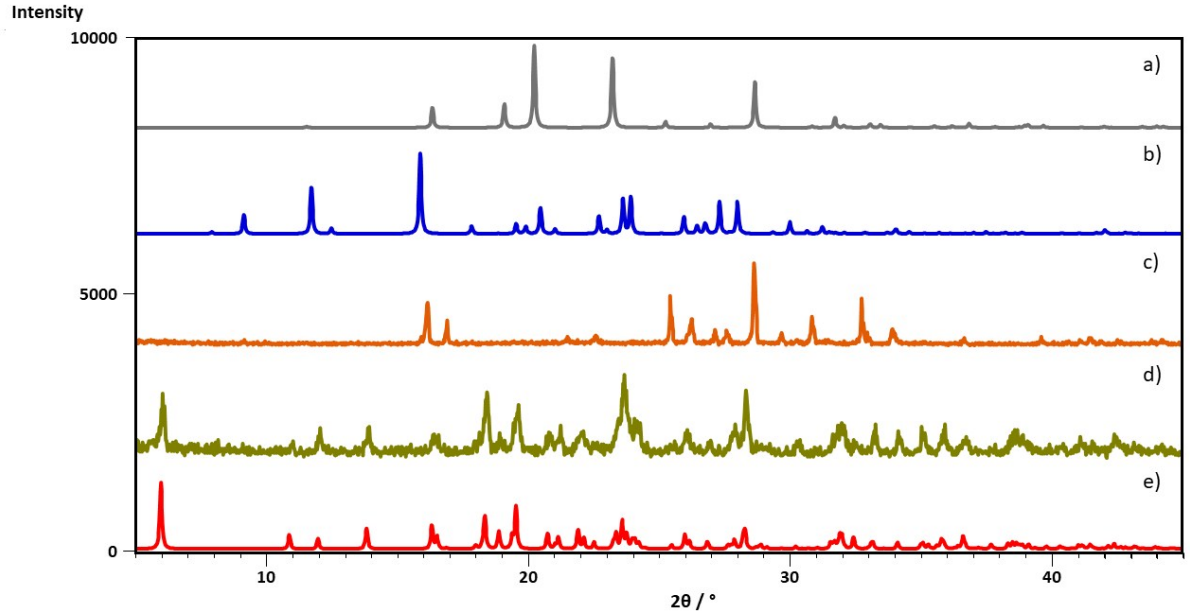

Figure S12 The PXRD patterns of a) **amp**, b) **II**, c) **14tfib**, d) the powder product of grinding **sal**, **amp** and **14tfib** (2:2:1) and e) the calculated PXRD pattern of **(II)$_2$(14tfib)**.

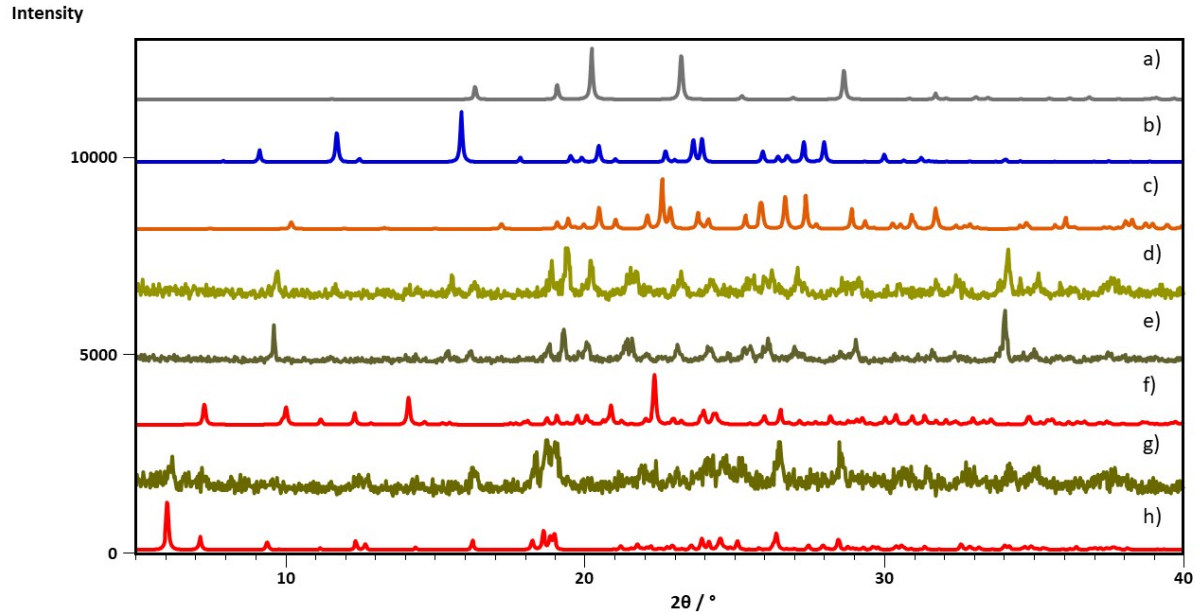

Figure S13 The PXRD patterns of a) **amp**, b) **II**, c) **135tfib**, d) the powder product of grinding **sal**, **amp** and **135tfib** (1:1:1), e) the powder product of grinding **sal**, **amp** and **135tfib** (1:1:1) with addition of **EtOH**, f) the calculated PXRD pattern of **(II)(135tfib)**, e) the powder product of grinding **sal**, **amp** and **135tfib** (2:2:1) and f) the calculated PXRD pattern of **(II)$_2$(135tfib)**.

3. Results of the thermal study

The results of the thermal study are summarized in Table S5 and Table S6. TG and DSC curves are shown in Figures S14 – S25.

Table S5 The results of TG analysis.

Cocrystal	t_1 / °C	t_2 / °C	%
(I)(14tfib)	91	262	85.9
(II)(12tfib)	78	334	87.5
(II)(13tfib)	69	293	64.5
$(II)_2$(14tfib)	112	354	78.2
(II)(135tfib)	124	339	73.3
$(II)_2$(135tfib)	170	307	46.3

Table S6 The results of DSC analysis.

Cocrystal	t_e / °C	ΔH / kJmol^{-1}
(I)(14tfib)	76	23.71
(II)(12tfib)	60	23.19
(II)(13tfib)	67	21.46
$(II)_2$(14tfib)	113	58.00
(II)(135tfib)	100	26.67
$(II)_2$(135tfib)	97	42.66

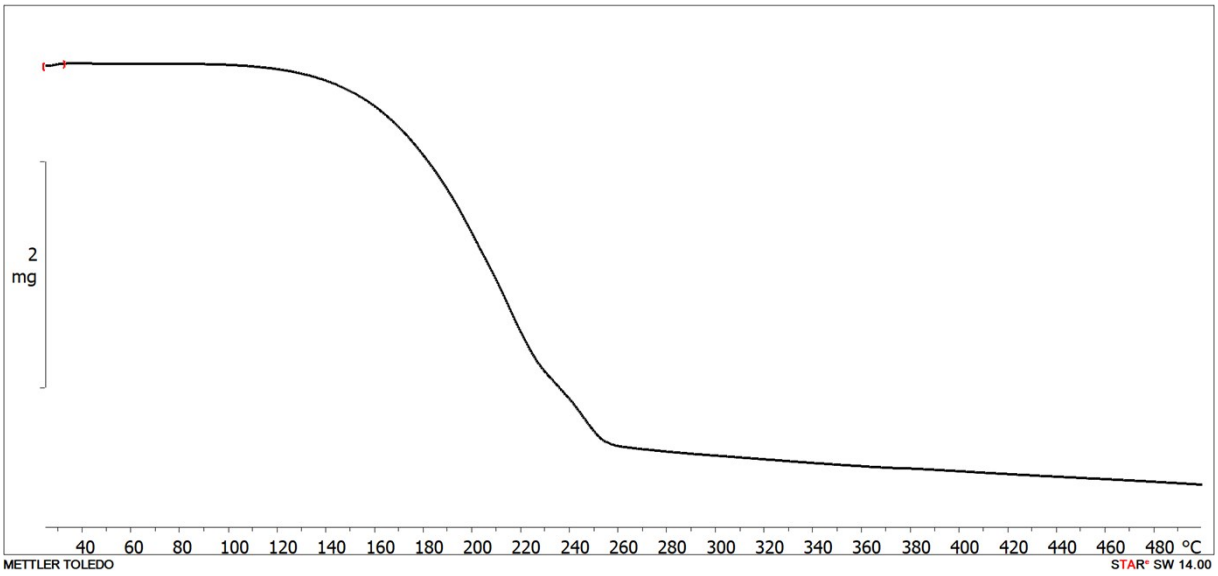

Figure S14 TG curve of the powder product of grinding **I** and **14tfib** (1:1).

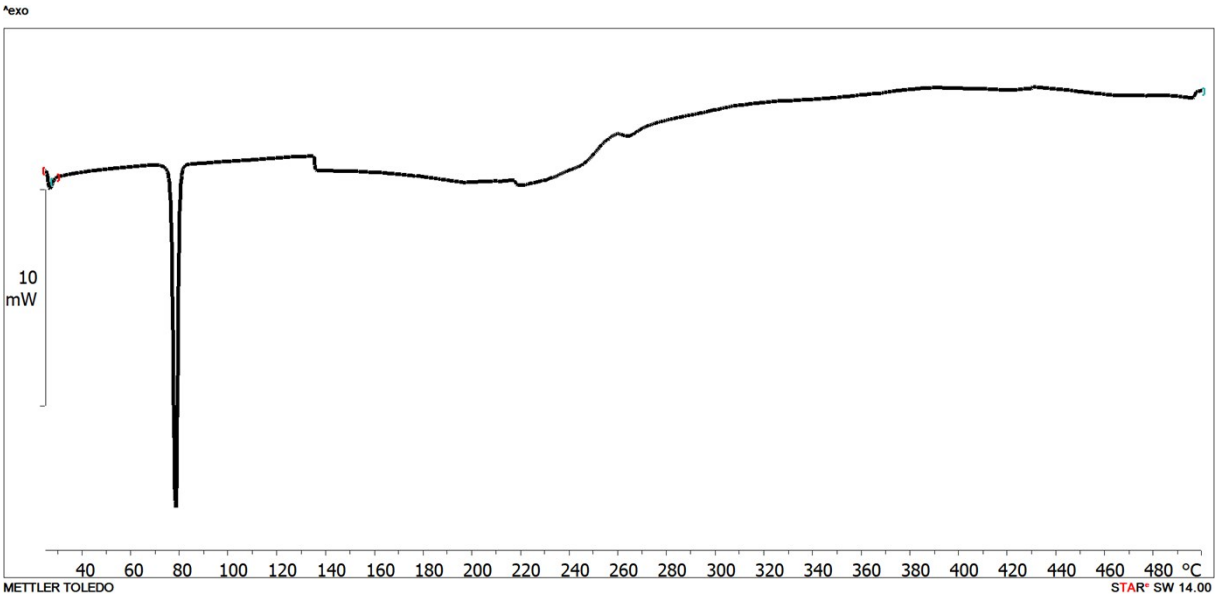

Figure S15 DSC curve of the powder product of grinding **I** and **14tfib** (1:1).

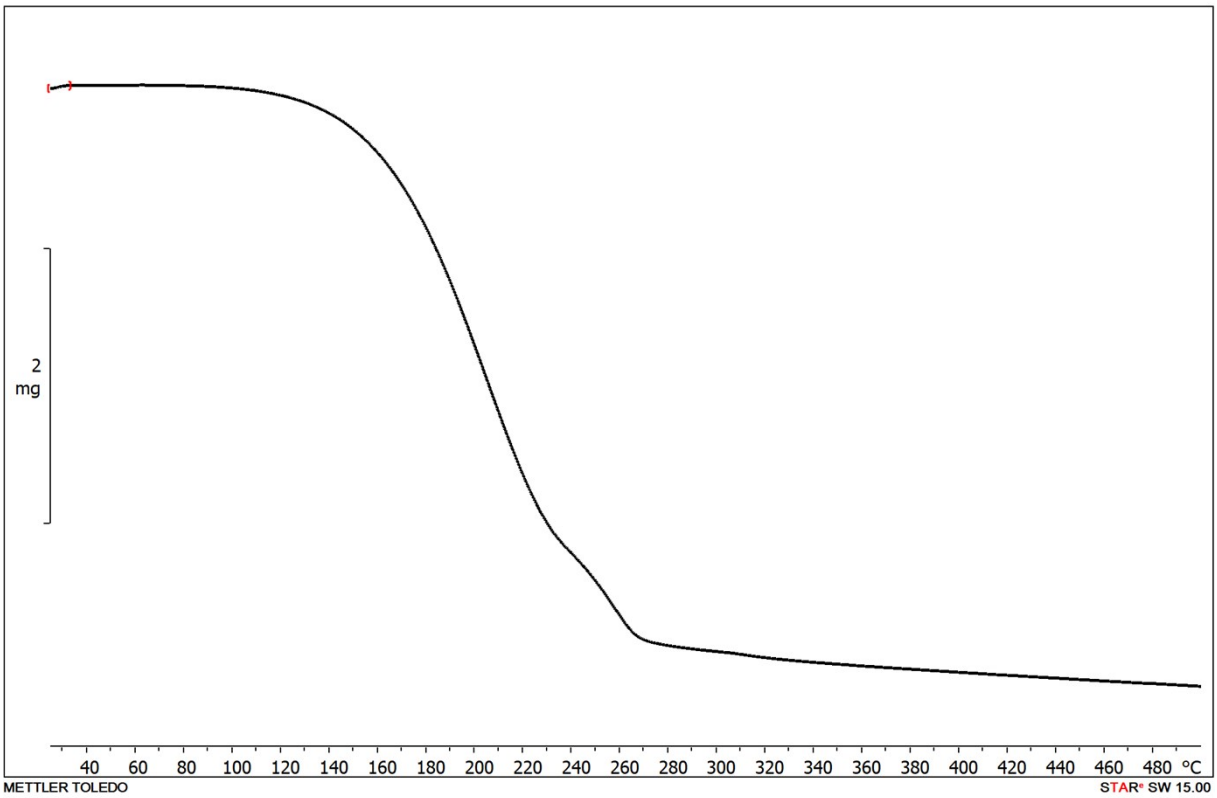

Figure S16 TG curve of the powder product of grinding **sal**, **amp** and **12tfib** (1:1:1).

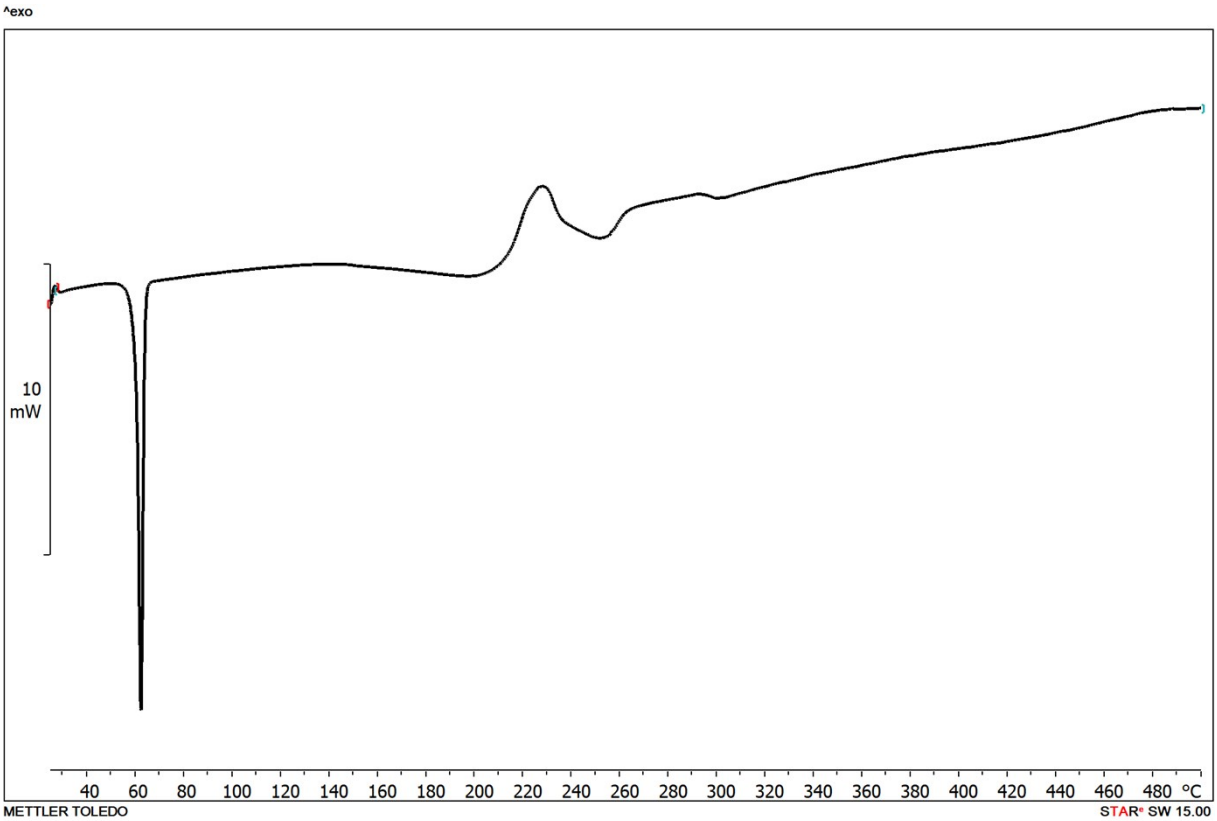

Figure S17 DSC curve of the powder product of grinding **sal**, **amp** and **12tfib** (1:1:1).

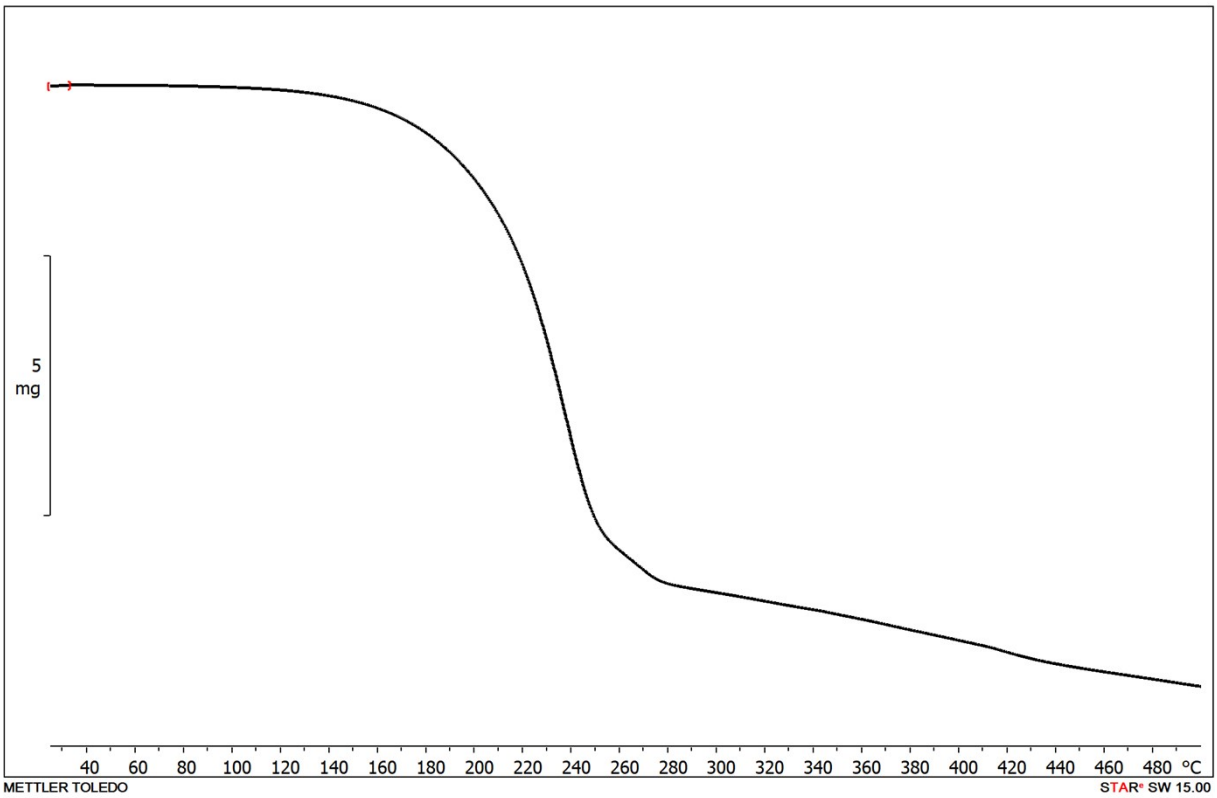

Figure S18 TG curve of the powder product of grinding **sal**, **amp** and **13tfib** (1:1:1).

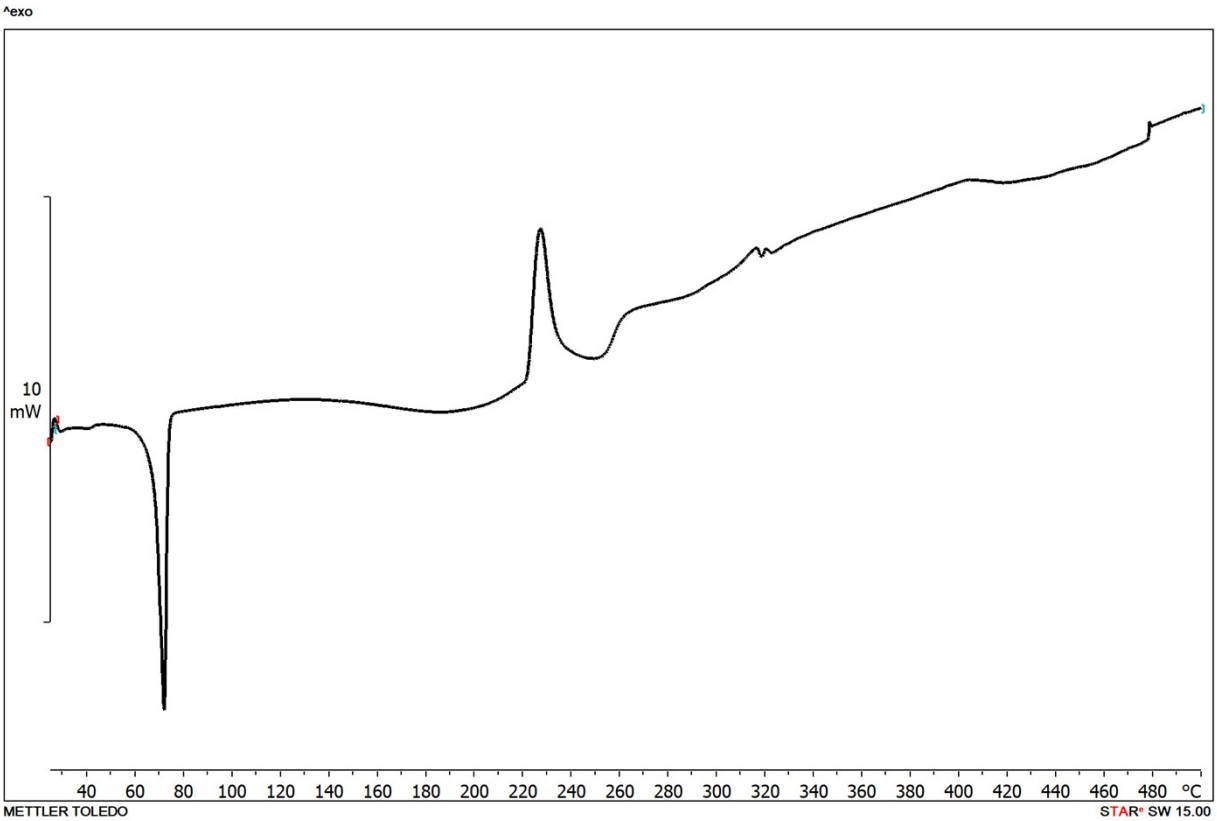

Figure S19 DSC curve of the powder product of grinding **sal**, **amp** and **13tfib** (1:1:1).

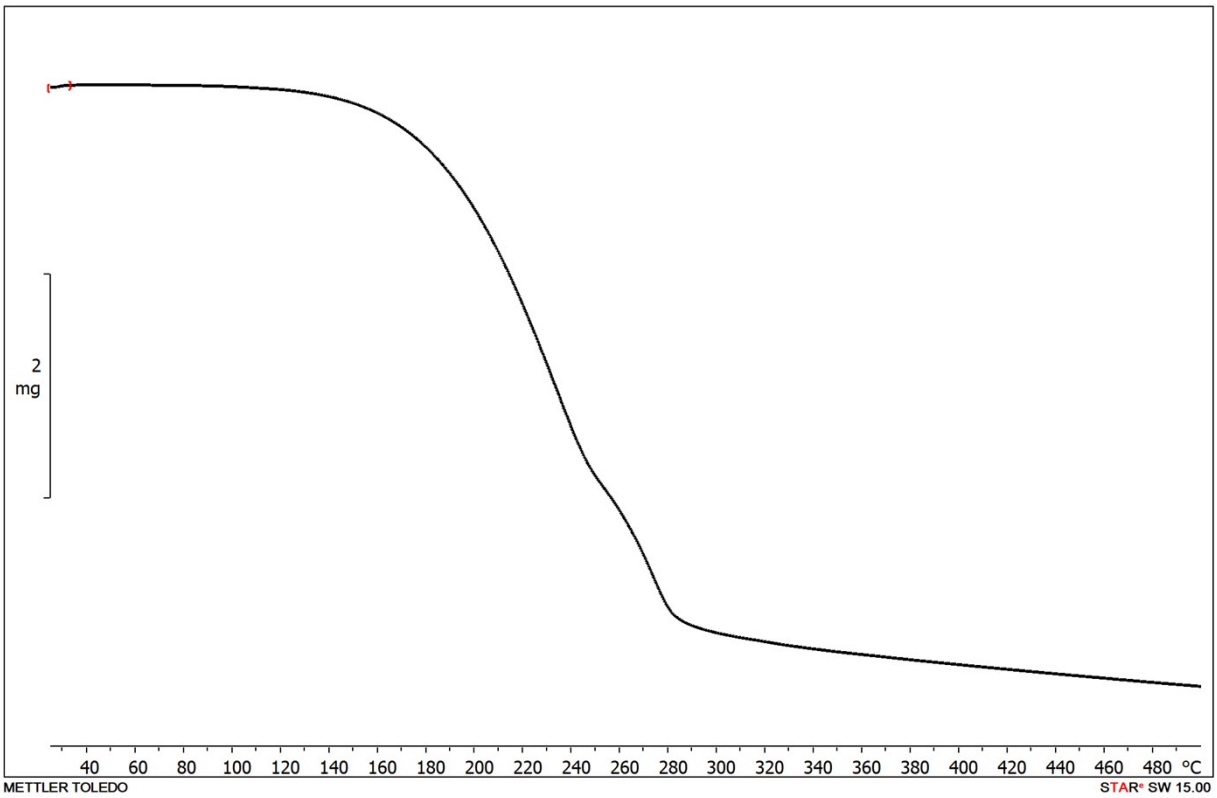

Figure S20 TG curve of the powder product of grinding **sal**, **amp** and **14tfib** (2:2:1).

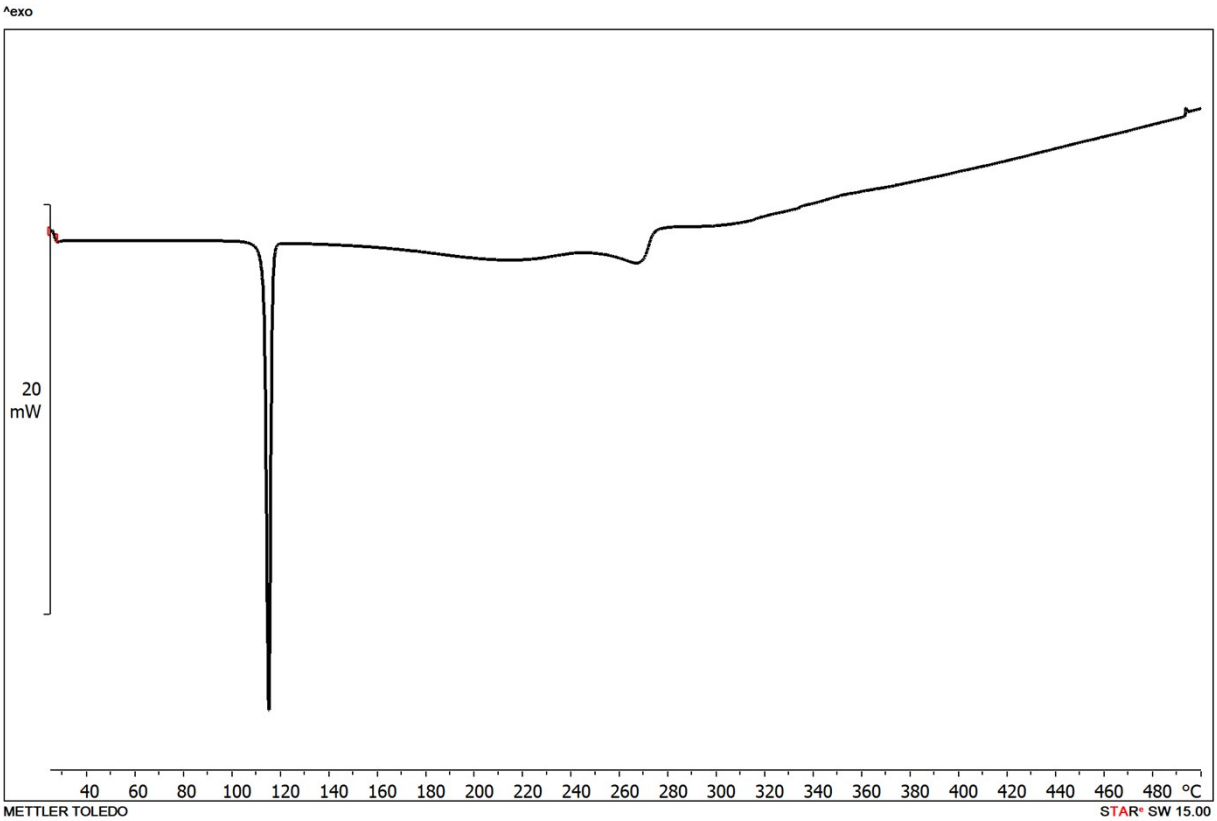

Figure S21 DSC curve of the powder product of grinding **sal**, **amp** and **14tfib** (2:2:1).

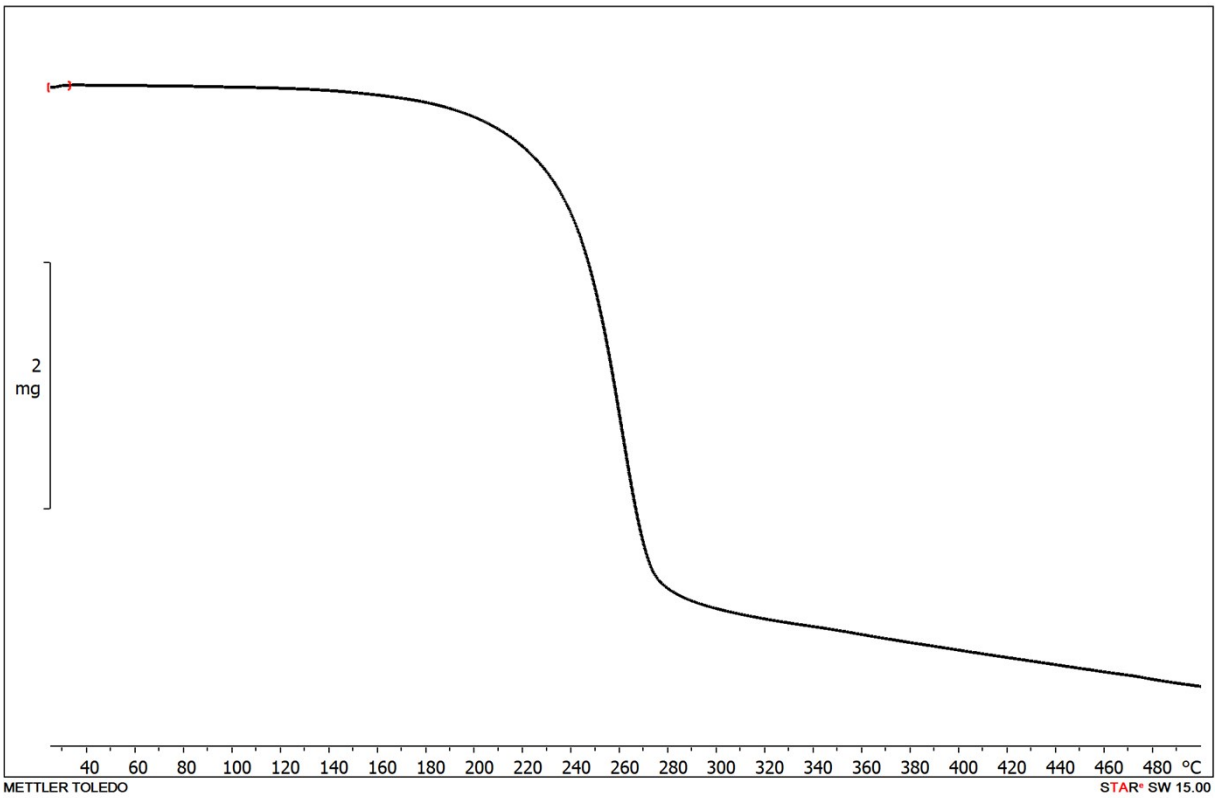

Figure S22 TG curve of the powder product of grinding **sal**, **amp** and **135tfib** (1:1:1).

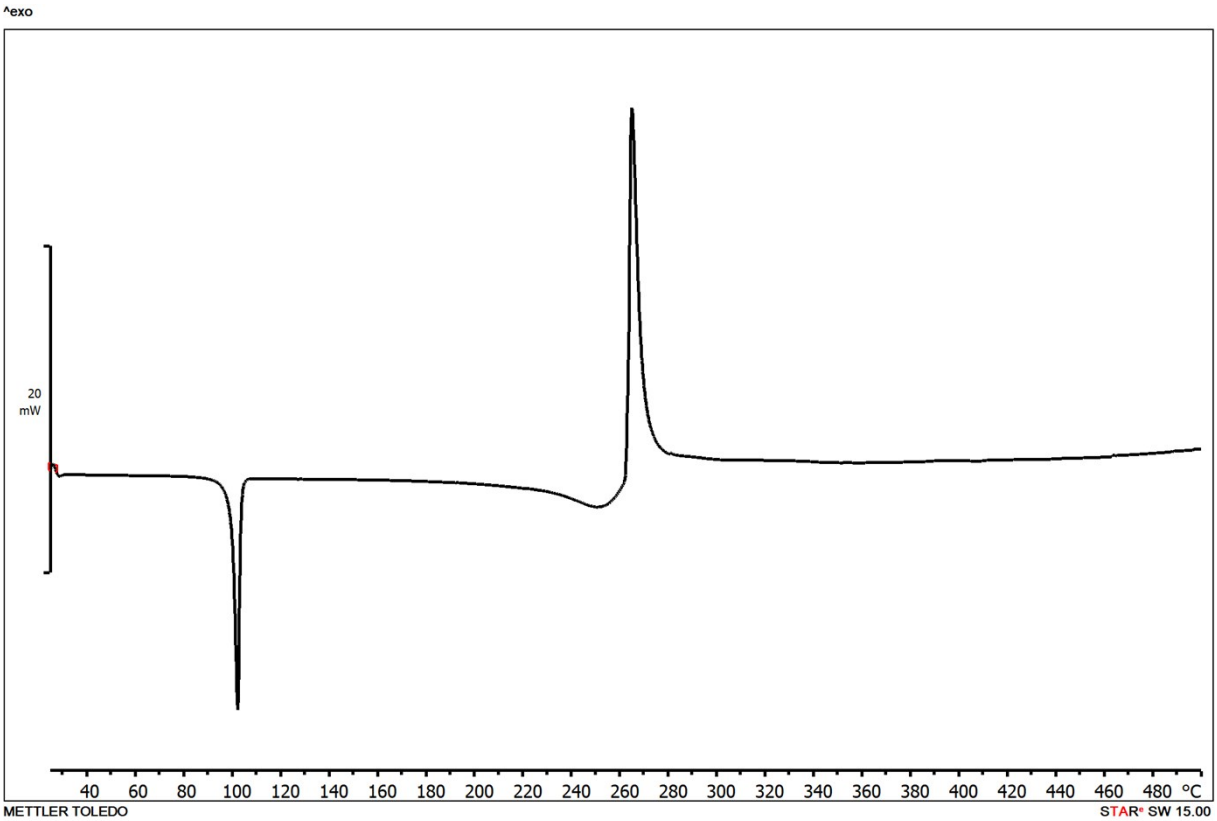

Figure S23 DSC curve of the powder product of grinding **sal**, **amp** and **135tfib** (1:1:1).

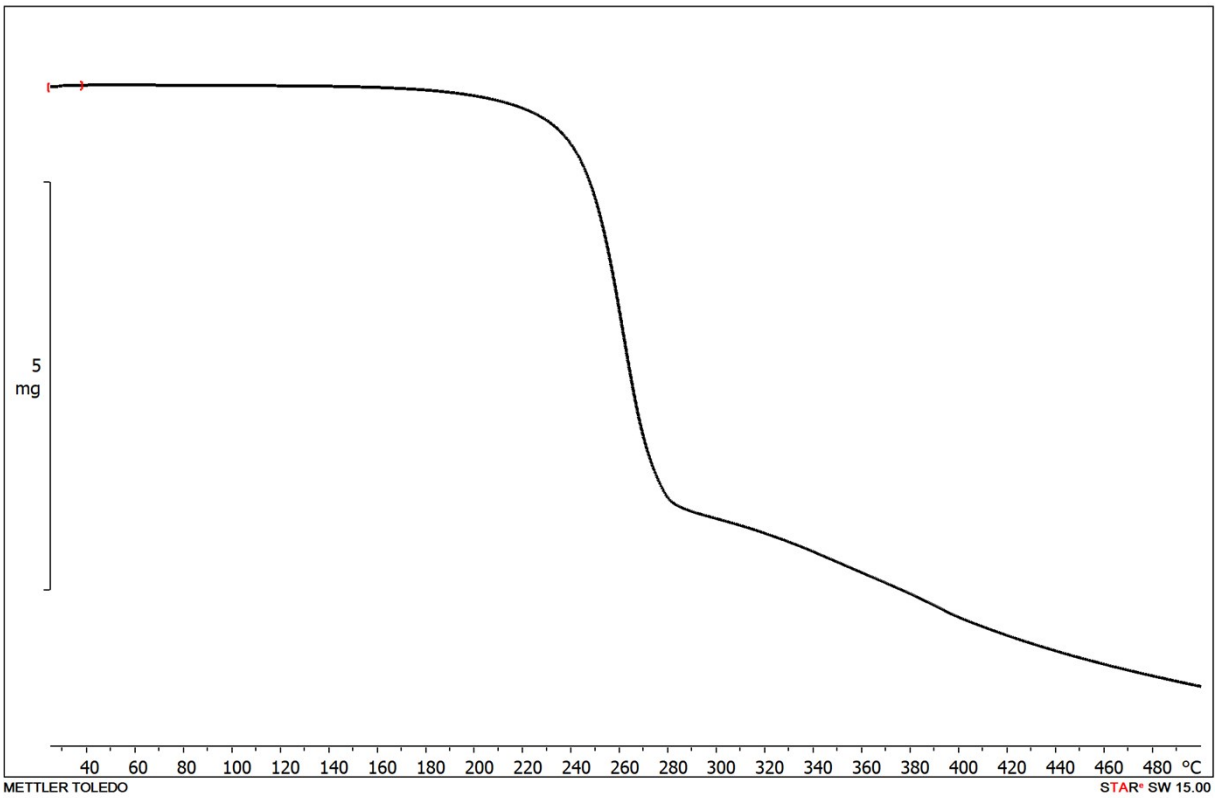

Figure S24 TG curve of the powder product of grinding **sal**, **amp** and **135tfib** (2:2:1).

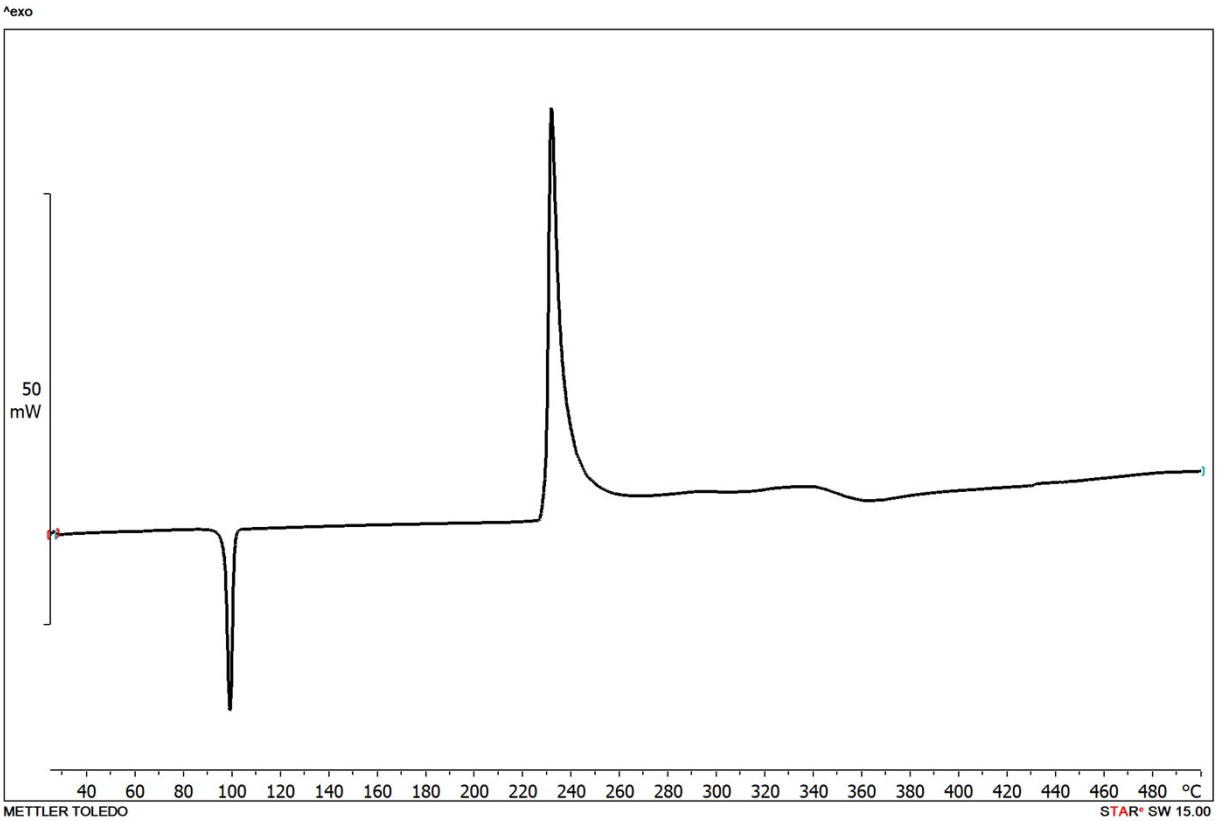

Figure S25 DSC curve of the powder product of grinding **sal**, **amp** and **135tfib** (2:2:1